Microfabrication and Evaluation of a Silicon Microelectrode Based on SOI Wafer*

Sui Xiaohong[1,†] and Chen Hongda[2]

(1 *Institute for Laser Medicine and Biophotonics, Department of Biomedical Engineering, Shanghai Jiao Tong University, Shanghai 200240, China*)

(2 *State Key Laboratory of Integrated Optoelectronics, Institute of Semiconductors, Chinese Academy of Sciences, Beijing 100083, China*)

Abstract: An implantable seven-channel silicon microelectrode was fabricated by MEMS (micro-electro-mechanical system) micromachining techniques for optic-nerve visual prosthesis applications. Theoretical analyses of noise contributed to determining the size of the exposed recording sites of the microprobe. The geometry configuration was optimized for the silicon microprobe to have enough strength and flexibility and to reduce the insertion-induced tissue trauma. Impedance test results showed that the average value of the channels was 2.3MΩ at 1kHz when applied with a stimulating voltage with the amplitude of 50mVpp, which is suitable for neural signal recordings. *In-vivo* animal experiment showed that the recorded neural signal amplitude from the primary visual cortex was 8μV.

Key words: MEMS; visual prosthesis; silicon microelectrode; *in-vivo* experiment
PACC: 0670D; 0710C; 7340 **EEACC**: 2110; 2550; 2575B
CLC number: TN303 **Document code**: A **Article ID**: 0253-4177(2008)11-2169-06

1 Introduction

Implantable microprobes or microelectrodes are key components for epiretinal[1,2], subretinal[3,4], suprachoroidal[5], visual cortical[6,7] and optic-nerve[8,9] visual prosthesis applications. At present, various scientific research groups contribute to these different kinds of visual prostheses and have produced some preliminary results for clinical applications. For optic-nerve visual restoration, microelectrodes are applied to stimulate optic nerves to restore vision for retinitis pigmentosa (RP) and age-related macular degeneration (AMD) patients. To realize the fundamental corresponding relationships between optic-nerve bundles and the primary visual cortex for pattern sensation, stimulation and recording microelectrodes are used for optic-nerve stimulation and cortical neural recording, respectively. Due to the millions of axons in the optic-nerve, rigid requirements are put forward for the optic-nerve stimulation and cortical recording microelectrodes.

Considerations for the implantable microelectrodes can be made from several aspects such as biocompatibility, tissue trauma, uniformity, and high yield. Metal microwires and silicon microelectrodes are usually selected as the neural interface for neural recording and stimulation. Metal microwires made of stainless steel, tungsten, and platinum were prevalent at the early stage of neural prosthesis applications. They were manufactured manually and had poor uniformity, low yield, and high cost. With the development of the micro-electro-mechanical system (MEMS) micromachining technique, silicon-based microelectrodes can be fabricated in batches and have satisfactory uniformity, high yield, and low cost. The silicon microelectrodes have relatively good flexibility and mechanical strength compared with silicon/silicon dioxide ones[10,11]. Si (silicon), SiO_2 (silicon dioxide), and Si_3N_4 (silicon nitride) are biocompatible with biological tissue and suitable for *in-vivo* application[12]. As a result, silicon-based microelectrodes have attracted much interest in recent years. Two and three-dimensional Michigan and Utah silicon microelectrodes have been fabricated[13~16]. The silicon microelectrodes or microprobes can be fabricated based on single-crystal silicon or silicon-on-insulator (SOI) wafers. Based on single-crystal silicon substrate, a deep p^{++} boron diffusion process is usually included to determine the outline of the silicon microelectrodes with higher concentration grads between the p^{++} layer and the silicon substrate. This presents rigid requirements for the diffusion process. In contrast, based on an SOI wafer, the top silicon or silicon device layer determines the thickness of the silicon microelectrode with precisely controlled uniformity. Moreover, the buried

* Project supported by the National Natural Science Foundation of China (No. 30700217)
† Corresponding author. Email: suixhong@sjtu.edu.cn
Received 26 March 2008, revised manuscript received 27 June 2008

SiO_2 layer is an etch stop layer while releasing the microelectrode. The fork-like microprobe based on SOI substrates was demonstrated by the double-sided deep reactive ion etching (DRIE) processing technique[17,18]. Double-sided photolithography and an additional mask for the base plate were introduced to obtain thin-film needle-shaped microprobes with a bonding pad area as thick as the original SOI wafer. The thicker base plate increased the weight and vertical dimension of the microprobes, and tissue dimpling may not be reduced effectively. In addition, the exposed recording sites were concave and not close enough to the neuron body or axon, which affected the neural recordings efficiency. Consequently, there is still room for the improvement of previous processes or designs.

Research on silicon-based microprobes from other groups mainly concentrates on the details of the fabrication process. By contrast, our work theoretically analyzes the noise to optimize the dimension of the stimulating sites, and a silicon microelectrode was fabricated based on SOI substrate with a uniform thickness of 15μm. The base plate was as thick as the probe shaft determined by the top silicon layer of the SOI wafer. The double-sided photolithography and one mask for the base plate were eliminated, and resulted in less tissue dimpling. A seven-channel silicon microprobe was fabricated for visual cortical recordings. The site size was optimized according to theoretical analysis results of thermal noise, and the impedance was on the order of MΩ at 1kHz. The outline design required that the silicon microprobe had a sharp side with a small lateral tip angle to reduce the insertion-induced tissue trauma. Processes and designs of the silicon microprobe based on SOI wafer were detailed in this paper. *In-vivo* animal experiment results showed that the microelectrode was feasible to record visual cortical neural signals for optic-nerve visual prosthesis applications.

2 Design and fabrication methodology

2.1 Noise analyses

The *in-vivo* neural recording setup is unavoidably affected by main-frequency disturbance, background noise, and thermal (Johnson) noise of the microelectrode. Disturbance from the main frequency can be eliminated by a shielded cover. The background noise results from respiration and excitation of thousands of neurons far from the exposed microelectrode sites and is closely related to the animal conditions, and so the thermal noise analysis is detailed here. After the microelectrode was implanted *in vivo*, the exposed metal sites were electrically related with physiological saline solution. The equivalent circuit of the metal-electrolyte interface[19] was illustrated in Fig. 1. R_{met} denoted the interconnecting metal wire resistance on the order of tens of ohms, and C_e and R_e denote the double-layer capacitance and resistance, respectively. E is the half-cell voltage at the metal-electrolyte interface.

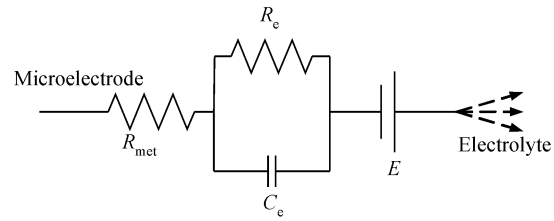

Fig. 1 Equivalent circuit of microelectrode-electrolyte interface

According to Fig. 1, thermal noise was dominated by R_{met}, R_e-C_e network. R_{met} and the resulting power spectral density (PSD) of thermal noise were shown in Eqs. (1) and (2), respectively.

$$R_{met} = \rho \times \frac{L}{S} \tag{1}$$

$$S(f) = 4kTR_{met} \tag{2}$$

where k ($= 1.38 \times 10^{-23}$ J/K) was the Boltzmann's constant, T was the absolute temperature in Kelvin, ρ is the gold resistivity with the value of 2.4×10^{-8} Ω·m, L was the connecting wire length of several millimeters, and S denoted the cross section area. In our design, L was selected as 6mm, S was 300nm × 5μm, and R_{met} was 96Ω. According to Eq. (2), $S(f) = 1.6 \times 10^{-18}$ V^2/Hz, and the equivalent thermal noise voltage was 1.3nVrms, which is neglected usually. Therefore, the noise is mainly produced from the R_e-C_e network shown in Fig. 2.

Figure 2 (a) showed the practical parallel network of a resistor and capacitor, and Figure 2 (b) shows the equivalent noise model of this network considering thermal noise from R_e. The dashed-line block denotes the ideal network. The PSD of R_e and the transfer function $h(f)$ were, respectively, expressed in Eqs. (3) and (4), the PSD of the output terminals $S_{out}(f) = S_v(f)|h(f)|^2$ was shown in Eq. (5), and the

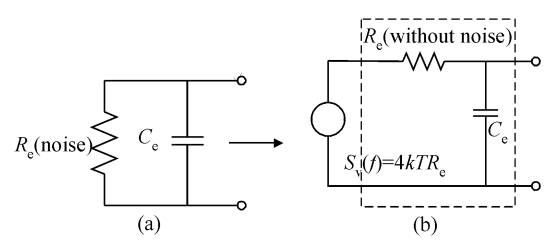

Fig. 2 Noise-analysis model of R_e-C_e network

total noise $P_{n,out}$ within the total frequency range was shown in Eq.(6).

$$S_v(f) = 4kTR_e \tag{3}$$

$$h(f) = \frac{1}{1 + j2\pi fR_eC_e} \tag{4}$$

$$S_{out}(f) = \frac{4kTR_e}{1 + 4\pi^2 R_e^2 C_e^2 f^2} \tag{5}$$

$$P_{n,out} = \int_0^\infty S_{out}(f)df = \frac{kT}{C_e} \tag{6}$$

where the unit of kT/C_e was V^2, and $(kT/C_e)^{1/2}$ was the equivalent noise voltage with the unit of Vrms. The equivalent noise voltage of the R_e-C_e network within the total frequency range was inversely proportional to C_e. With settled temperature, increasing C_e reduced the thermal noise voltage, which increased the site area for the multichannel microelectrode with planar metal sites exposed. At a body temperature of 310K, the equivalent thermal noise voltage at the total frequency range was 65.4μVrms with a C_e of 1pF.

Thermal noise analyses resulted in the size selection of the exposed planar site, and the impedance Z was mainly determined from R_e and C_e in Eq.(7).

$$Z = \frac{R_e}{1 + j2\pi fR_eC_e} \tag{7}$$

In view of Eqs.(6) and (7), low thermal noise meaned a large signal-to-noise ratio (SNR), a large site size, low impedance, and low spatial resolution.

To achieve high spatial resolution, microelectrodes for neural spike recording had a site size comparable to the neuron body, which introduced large impedance on the order of MΩ with relatively large noise voltage. The site size must be compromised to satisfy the requirements of low thermal noise (high sensitivity) and high spatial resolution (high selectivity).

2.2 Fabrication process technology

Compared with the Si/SiO_2 microelectrode based on silicon substrate, the silicon one was fabricated on SOI substrate. The original SOI wafer was manufactured by a bonding technique with a top silicon layer of 15μm, a buried silicon dioxide layer of 1μm, and a silicon base plate of 500μm. The fabrication process was as follows: (1) Lower 300nm silicon nitride layer was deposited on the SOI wafer by plasma enhanced chemical vapor deposition (PECVD)[9] to electrically separate the top silicon of the SOI wafer and metal connecting wires. (2) Lower titanium/gold (Ti/Au) of 100nm/300nm was sputtered on the lower silicon dioxide successively and patterned as conductor traces by diluted buffered oxide etching (BOE) and gold corrosive, respectively. Then, the probe was annealed at 380℃ for 40min. (3) Upper 300nm SiO_2 was deposited by PECVD to insulate the metal layer from the tissue solution. (4) The upper SiO_2 layer was etched by BOE to open Φ-6μm contact holes near the tip and bond pads at the rear. (5) According to step (2), seven Φ-10μm circular recording sites were formed with the central space of 120μm. (6) A thick photoresist was used as the mask layer, and the horizontal architecture of the microelectrode was determined by the ICP (inductively-coupled plasma) dry etching process technique. (7) The wafer was thinned to 200μm by physical ablation of the bottom silicon and adhered to plane glass plate by black wax. Then the wafer was further thinned to 50μm by BOE solution. (8) After removing the wax, the top side of the wafer was protected and adhered to another silicon wafer by a photoresist. The bottom silicon layer of the wafer was plasma dry etched using SF_6. Because of the low selectivity ratio between silicon and silicon dioxide, the buried silicon dioxide layer was removed at the same time. Consequently, the individual silicon microelectrodes were accomplished after the photoresist-removing techniques by acetone.

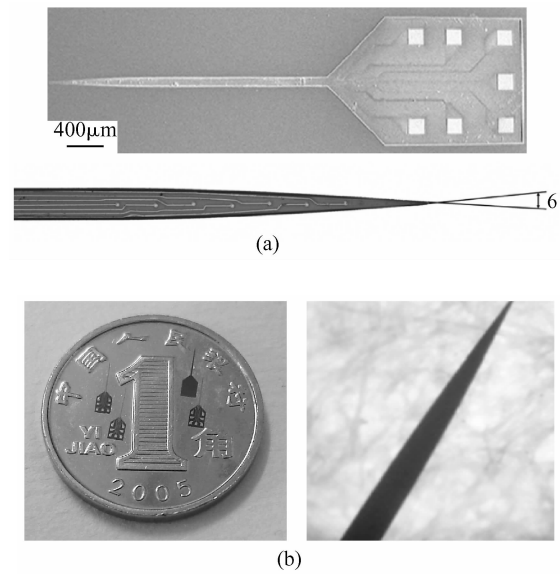

Fig.3　Silicon microelectrode based on SOI wafer　(a) SEM picture of the microelectrode top view after ICP process　The probe shank was 3mm long with a 6° tip angle, and the exposed seven circle recording sites were 10μm in diameter; (b) Picture of released individual silicon microelectrodes with the top and back sides shown: the tip was sharp and arc-shaped

Figure 3 showed the pictures of the silicon microelectrode.

3 Evaluation and discussion

3.1 Noise and impedance characteristics

To increase the spatial resolution, the size of the recording sites should be as small as possible. Small

Table 1 Tested capacitance C_e of the seven-channel microelectrode

Recording site 1/pF	Recording site 2/pF	Recording site 3/pF	Recording site 4/pF
60	69	58	64
Recording site 5/pF	Recording site 6/pF	Recording site 7/pF	Average /pF
60	69	58	62.5

Table 2 Tested impedances of the seven-channel microelectrode

Recording site 1/ MΩ	Recording site 2/MΩ	Recording site 3/MΩ	Recording site 4/MΩ
2.5	1.49	2.65	2.3
Recording site 5/MΩ	Recording site6/MΩ	Recording site 7/MΩ	Average / MΩ
2.5	1.49	2.65	2.3

site area meaned large noise voltage and large impedance. To compromise the noise voltage and spatial resolution, the site size was optimized as 10μm in diameter, comparable to a neural cell body. According to Eq. (6), the thermal noise voltage was proportional to the square root of C_e. In our experiment, C_e was tested in 0.9% saline solution in a stainless cup by a IMP-1 LCR Meter (BAK ELECTRONICS, Inc.).

With the temperature of 310K and C_e of 62.5pF, the resulting thermal noise voltage was 2.61μVrms. This value was much smaller than the neural signals on the order of tens to hundreds of μV. In order to further reduce the noise, some measures could be adopted to rough the site surface without changing the dimension.

Impedance had a direct relationship with site area and the spatial resolution. As a result, impedance evaluation became a common method to non-invasively determine the electrical continuity and conditions of chronically implanted microelectrodes *in-vivo*. Since electrophysiological saline solution was the primary constituent of body fluids, it was generally assumed as the impedance-testing environment *in-vivo*.

The impedance Z was tested under the same conditions as C_e. Two terminals of the impedance spectrometer were connected to one channel of the silicon-based microelectrode and the stainless cup, respectively. The channel impedances at 1kHz were displayed in Table 1, and the results showed that the impedance was on the order of MΩ with an applied voltage amplitude of 50mVpp. The average impedance value was 2.3MΩ, which was ideal for neural recordings.

3.2 *In-vivo* experiment

Rabbits were selected as the experiment animals, and proper animal surgery was adopted to expose the optic nerve and the primary visual cortex. The rabbits

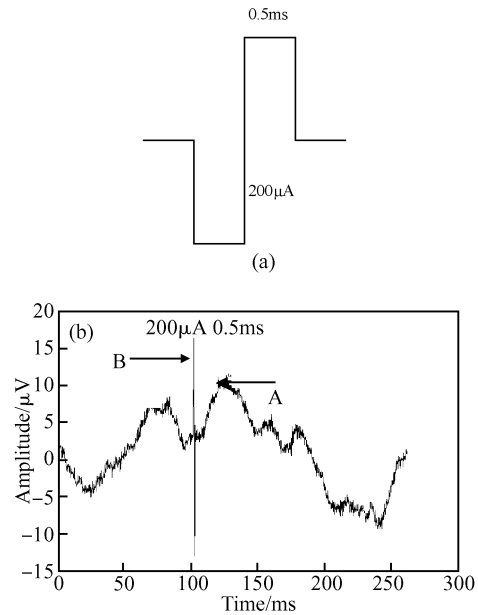

Fig. 4 (a) Stimulating microcurrent pulse; (b) EEP signal from primary visual cortex recorded by the silicon microprobe

were anesthetized with intravenous injection of 3% pentobarbital sodium (30mg/kg). After the skin of external canthus was dissected, conjunctiva and sub-Tenon space was opened at the limbus under a surgical microscope. The lateral rectus muscle was found and then snipped. Microsurgical forceps were used to expose the optic nerve near the eyeball. The contralateral visual cortex pia was also exposed.

Although the platiridium microelectrode was manually made with unsatisfactory uniformity and low yield, it was selected to stimulate the optic nerve in our work because of its favorable mechanical strength, stable electrochemical characteristics, and good biocompatibility.

Two Φ-85μm platiridium microwires were inserted to the optic nerve bundles and formed the stimulation circuit loop. The silicon microelectrode was implanted to the primary visual cortex to record neural signals with the reference electrode on the skull. Then, when stimulating microcurrent was applied to the platiridium microwires, the corresponding electrical evoked potential (EEP) signals could be picked up by the multichannel silicon microelectrode. Figure 4 shows the relationship between stimulating and recording signals. The stimulating microcurrent waveform between two microwires is shown in Fig. 4 (a), and the resulting signal recorded by silicon microelectrode is shown in Fig. 4 (b).

Signals A and B in Fig. 4 (b) were the recorded EEP and wake signal, respectively, and the former was about 8μV in amplitude. The response region of the visual cortex was small considering the size of the stimulating microwires. As a result, when the silicon

microelectrode was a little far from the response region, the EEP amplitude was relatively low. In order to effectively localize the response region, a silicon microelectrode array with more shanks and channels will be used.

4 Conclusion

Multichannel silicon microelectrodes were fabricated based on SOI wafers for optic-nerve visual prosthesis. Owing to the sandwich structure, the top silicon layer was used as the main body and determined the thickness of the microelectrode. According to the theoretical analyses of thermal noise, the site size was decided for recording purposes, and so was the impedance. The details of the fabrication process were described and pictures of the fabricated silicon microelectrodes were shown. With a lateral tip angle of 6° and a sword-shaped outline, the induced tissue trauma can be reduced greatly. The bonding pad area was as thick as the probe shank, which can reduce the tissue dimpling and aids in chronic neural recordings. The Φ-10μm circular recording sites protrude to form a close relationship with the outside electrolyte or neurons. The acute *in-vivo* animal experiment showed that the silicon microelectrode was feasible for neural recordings.

To further determine the preliminary relationship between optic nerve and primary visual cortex for optic nerve visual restoration, a 3D silicon microelectrode array with more channels and probe shanks will be fabricated.

Acknowledgements The authors would like to acknowledge Cai Changsi and Li Xiaoliang for their kind assistance with the *in-vivo* animal experiment. They also would like to thank Doctor Pei Weihua for his technical support at the Institute of Semiconductors, Chinese Academy of Sciences.

References

[1] Koury C B. Epiretinal prosthesis shows promise for blind patients. Retina Today, 2006, (12): 38

[2] Humayun M S, Weiland J D, Fujii G Y, et al. Visual perception in a blind subject with a chronic microelectronic retinal prosthesis. Vision Research, 2003, 43: 2573

[3] Chow A Y, Chow V Y, Packo K H, et al. The artificial silicon retina microchip for the treatment of vision loss from retinitis pigmentosa. Archives of Ophthalmology, 2004, 122: 460

[4] Chow A Y, Pardue M, Chow V Y, et al. Implantation of silicon chip microphotodiode arrays into the cat subretinal space. IEEE Trans Neural Systems and Rehabilitation Engineering, 2001, 9: 86

[5] Kanda H, Morimoto T, Fujikado T. Electrophysiological studies of the feasibility of suprachoroidal-transretinal stimulation for artificial vision in normal and RCS rats. IOVS, 2004, 45(2): 560

[6] Troyk P, Bak M, Berg J, et al. A model for intracortical visual prosthesis research. Artificial Organs, 2003, 27: 1005

[7] Brindley G S, Lewin W S. The sensations produced by electrical stimulation of the visual cortex. Journal of Physiology, 1968, 196: 479

[8] Jean Delbeke M O, Veraart C. Position, size and luminosity of phosphenes generated by direct optic nerve stimulation. Vision Research, 2003, 43: 1091

[9] Claude Veraart C R, Thomas Mortimer J, Delbeke J, et al. Visual sensations produced by optic nerve stimulation using an implanted self-sizing spiral cuff electrode. Brain Research, 1998, 813: 181

[10] Sui Xiaohong, Pei Weihua, Zhang Ruoxin, et al. A micromachined SiO_2/silicon probe for neural signal recordings. Chinese Physics Letters, 2006, 23: 1932

[11] Sui Xiaohong, Zhang Ruoxin, Pei Weihua, et al. A novel implantable multichannel silicon-based microelectrode. Chinese Physics, 2007, 16: 2116

[12] Voskerician G, Shive M S, Shawg R S, et al. Biocompatibility and biofouling of MEMS drug delivery devices. Biomaterials, 2003, 24 (11): 1959

[13] Normann R A, Maynard E M, Rousche P J, et al. A neural interface for a cortical vision prosthesis. Vision Research, 1999, 39: 2577

[14] Mohseni P, Najafi K. A fully integrated neural recording amplifier with DC input stabilization. IEEE Trans Biomed Eng, 2004, 51 (5): 832

[15] Akin T, Najafi K, Bradley R M. A wireless implantable multichannel digital neural recording system for a micro-machined sieve electrode. IEEE J Solid-State Circuits, 1998, 33: 109

[16] Obeid I, Morizio J C, Moxon K A, et al. Two multichannel integrated circuits for neural recording and signal processing. IEEE Trans Biomed Eng, 2003, 50: 255

[17] Norlin P, Kindlundh M, Mouroux A, et al. A 32-site neural recording probe fabricated by DRIE of SOI substrates. J Micromech Microeng, 2002, 12: 414

[18] Cheung K C, Djupsund K, Dan Y, et al. Implantable multichannel electrode array based on SOI technology. J Microelectromechan Syst, 2003, 12: 179

[19] Daniel M B, Merrill R, Jefferys J G R. Electrical stimulation of excitable tissue: design of efficacious and safe protocols. Journal of Neuroscience Methods, 2004, 141: 171

基于 SOI 硅片的硅微电极制作与评估*

隋晓红[1,†] 陈弘达[2]

(1 上海交通大学生物医学工程系 激光与光子生物医学研究所，上海 200240)
(2 中国科学院半导体研究所 集成光电子学国家重点联合实验室，北京 100083)

摘要：采用微机电系统(MEMS)工艺方法制作了基于 SOI 衬底的七通道硅微电极，用于视神经视觉修复.通过噪声分析确定了硅微电极的金属暴露位点的几何尺寸.优化设计了硅微电极的几何结构，以便于减小植入损伤.阻抗测试结果表明，当测试电压为 50mVpp 时，1kHz 频率下，微电极的单通道阻抗为 2.3MΩ，适用于神经电信号记录.在体实验结果表明，动物初级视皮层记录到的神经电信号幅度为 8μV.

关键词：MEMS；视觉修复；硅微电极；在体试验
PACC：0670D；0710C；7340 **EEACC**：2110；2550；2575B
中图分类号：TN303 **文献标识码**：A **文章编号**：0253-4177(2008)11-2169-06

* 国家自然科学基金资助项目(批准号：30700217)
† 通信作者.Email：suixhong@sjtu.edu.cn
2008-03-26 收到，2008-06-27 定稿